Master Integrals for Massless Three-Loop Form Factors: One-Loop and Two-Loop Insertions

T. Gehrmann, G. Heinrich, T. Huber and C. Studerus

Institut für Theoretische Physik, Universität Zürich, Winterthurerstrasse 190, CH-8057 Zürich, Switzerland

Abstract

The three-loop form factors in massless QCD can be expressed as a linear combination of master integrals. Besides a number of master integrals which factorise into products of one-loop and two-loop integrals, one finds 16 genuine three-loop integrals. Of these, six have the form of a bubble insertion inside a one-loop or two-loop vertex integral. We compute all master integrals with these insertion topologies.

1 Introduction

The vertex functions of a virtual photon coupling to a quark-antiquark pair (quark form factor) and of a Higgs boson coupling to two gluons through an effective coupling (gluon form factor) are the simplest diagrams containing infrared divergencies in higher orders in massless quantum field theory. These form factors appear in a wide variety of applications: they can be used to predict the infrared pole structure of multi-leg amplitudes at a given order [1, 2] and to extract resummation coefficients [3], and they make up the purely virtual corrections to a number of collider reactions (Drell-Yan process, Higgs production and decay, deep inelastic scattering).

In the past, two-loop corrections to the massless quark [4] and gluon [5, 6] form factors were computed in dimensional regularisation in $D = 4 - 2\epsilon$ dimensions to order ϵ^0. Two-loop corrections to this order were also obtained for massive quarks [7]. The massless two-loop form factors were extended to all orders in ϵ in [8], and three-loop form factors to order ϵ^{-1} (and ϵ^0 for fermion loop contributions) were computed in [3, 9]. These three-loop results had an immediate application in the calculation of the N^3LO threshold-enhanced soft emission corrections [10] to the inclusive Drell-Yan and Higgs production cross section, demonstrating the perturbative stability at this order.

In [3, 9], the form factors were inferred from the behaviour of the three-loop deep inelastic coefficient functions [11]; this procedure can not be easily extended to yield also all the finite terms. Instead, one can turn to the more conventional approach of computing multi-loop Feynman amplitudes, which proceeds through a reduction [12–14] of all Feynman integrals appearing in the form factors to a small set of master integrals. The reduction is purely algebraic and can be automated using computer algebra methods [13, 15]. The master integrals take the form of a Laurent series in ϵ, and they must be computed to a given order in ϵ, typically specified by the transcendentality of the coefficients. The finite part of the three-loop form factors requires transcendentality six, i.e. coefficients containing terms up to π^6 or ζ_3^2.

In this letter, we identify all master integrals needed for the three-loop form factors in Section 2. Many of these are products of integrals with one or two loops, or three-loop propagator integrals. Among the remaining genuine three-loop vertex integrals, several contain one-loop or two-loop propagator insertions. We describe how the Laurent expansion of these insertion topologies can be obtained either analytically or numerically in Section 3, and list the results for them in Section 4. Finally, Section 5 contains our conclusions and an outlook.

2 Master integrals for three-loop form factors

The topologies of the master integrals relevant to three-loop form factors can be inferred from two-particle cuts of the master integrals of massless four-loop off-shell propagator integrals (massless four-loop two-point functions). The master integrals of these massless four-loop two-point functions were identified in [16] and subsequently used in the calculation of the scalar R-ratio [17]. Analytical expressions for these integrals are, however, not available in the literature. Since each two-particle cut is in general only one of several (two-, three-, four- and five-particle) cuts, knowledge of these two-point master integrals would not facilitate the calculation of the master integrals for the three-loop form factors.

These master integrals can be classified into three types: (i) products of one-loop and two-loop vertex functions with one off-shell and two on-shell legs, (ii) three-loop two-point functions, (iii) three-loop vertex functions with one off-shell and two on-shell legs. Since the one-loop and two-loop vertex functions are known to all orders in ϵ [8], all master integrals of type (i) can be obtained directly by expansion [18, 19] of the all-orders results. Likewise, three-loop two-point functions appearing in type (ii) are known to sufficiently high orders in ϵ [12, 20] and are tabulated for example in the MINCER package [21]. The only non-trivial master integrals for three-loop form factors are therefore of type (iii). The full set of these integrals is displayed in Figure 1. Each topology contains only one master integral, which is chosen to be the scalar integral, with no loop momenta in the numerator and with all propagators raised to unit power. Nevertheless, we will give the results for the two-loop insertions for arbitrary propagator powers, see Section 4. The topologies $A_{5,2}$ and $A_{6,2}$ with some of the lines being massive have been calculated in [22], where they enter the calculation of the three-loop matching coefficient of the heavy quark current.

Among the master integrals of Figure 1, the integrals $A_{5,1}$, $A_{5,2}$, $A_{6,1}$, $A_{6,3}$, $A_{7,1}$, $A_{7,2}$ are of special character, since they contain either a one-loop two-point insertion into a two-loop vertex integral ($A_{6,3}$, $A_{7,1}$, $A_{7,2}$) or a two-loop (or one-loop times one-loop) two-point insertion into a one-loop vertex integral ($A_{5,1}$, $A_{5,2}$, $A_{6,1}$). These so-called insertion topologies are in general simpler than the remaining genuine three-loop vertex integrals, since they can be obtained by computing a one-loop or two-loop vertex function with one or two propagators raised to a symbolic power. In the following, we describe the calculation of these insertion topologies.

3   Computational methods

Three-loop vertex integrals with one off-shell and two on-shell legs and massless propagators depend only on one kinematical scale: the mass q^2 of the off-shell leg. The dependence on this scale is given by the mass dimension of the integral, such that the coefficients of the Laurent expansion are constants, i.e. real numbers (which are in general of increasing transcendentality). Several techniques exist to compute such single-scale integrals.

For all one-loop and two-loop insertion topologies considered here, we performed two independent calculations, using two different techniques: evaluation in terms of hypergeometric series from Feynman parametrisation and evaluation using sector decomposition.

The Feynman parametrisation for the one-loop and two-loop vertex functions with symbolic powers on individual propagators results in a multiple integral in the Feynman parameters. Depending on the topology, one has to integrate over at least two (one-loop vertex function) and at most five (non-planar two-loop vertex function) Feynman parameters. After appropriately decomposing the integration region to avoid parametric singularities [23], and introducing supplementary regulators at intermediate stages, one can express the results of this integration in terms of hypergeometric functions of unit argument, containing ϵ-dependent coefficients. These can be expanded in ϵ using the `Mathematica` [24] package `HypExp` [18] to yield the Laurent series of the master integrals.

For many practical applications, and to verify the analytical results, it is sufficient to know the numerical values of the coefficients in the Laurent expansion of the master integrals to some

$A_{5,1}$ $A_{5,2}$ $A_{6,1}$ $A_{6,2}$

$A_{6,3}$ $A_{7,1}$ $A_{7,2}$

$A_{7,3}$ $A_{7,4}$ $A_{7,5}$

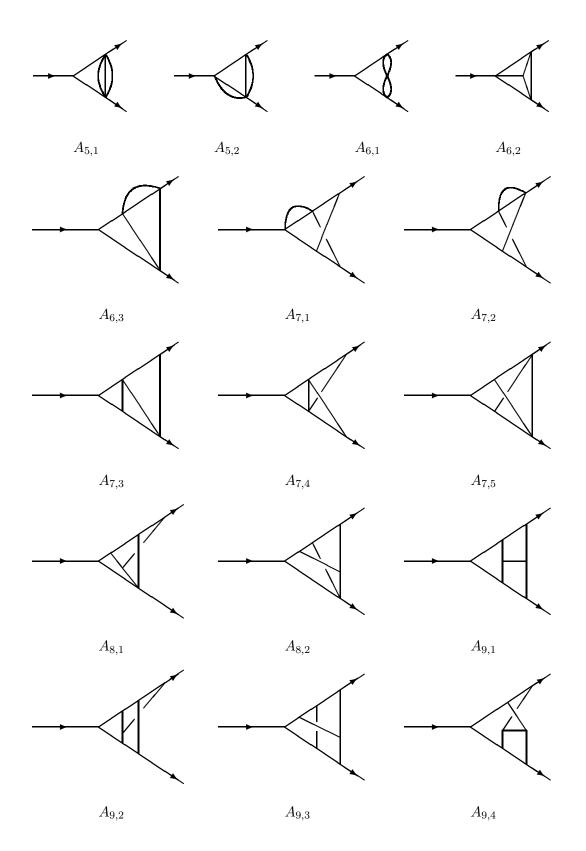$A_{8,1}$ $A_{8,2}$ $A_{9,1}$

$A_{9,2}$ $A_{9,3}$ $A_{9,4}$

Figure 1: Three-loop master integrals with massless propagators. The incoming momentum is $q = p_1 + p_2$. Outgoing lines are considered on-shell and massless, i.e. $p_1^2 = p_2^2 = 0$.

finite order. These can be obtained using the sector decomposition technique.

The sector decomposition technique for the computation of multi-loop integrals is described in detail in [25,26]. Using this technique, the Laurent expansions of all master integrals relevant to the three-loop form factors can be computed to any desired order, limited only by computation time. First applications to three-loop vertex integrals were presented already in [25]. The treatment of propagator powers different from unity is described in [26]. The application of sector decomposition to the topologies $A_{6,3}$, $A_{7,1}$ and $A_{7,2}$ has been done in two different ways: (a) by direct calculation of the three-loop topologies, (b) by calculating the two-loop diagram with ϵ-dependent propagator powers resulting from integrating out the one-loop two-point insertion (corresponding to $I_5(\epsilon)$, $I_6(\epsilon)$, $J_6(\epsilon)$ in Section 4). The analytical results for $A_{5,1}$, $A_{5,2}$ and $A_{6,1}$, given for general symbolic propagator powers ν_i in Section 4, also have been verified for some ϵ-dependent ν_i values by sector decomposition.

The computing time for a seven propagator graph like $A_{7,1}$ or $A_{7,2}$ up to order ϵ^0 for a numerical precision better than 0.1% is of the order of 20 minutes on a 2.8 GHz PC, while the order ϵ term takes about 6 hours. For a precision of 1% the evaluation is about 10 times faster.

4   Results for the insertion topologies

In this section we list the results we obtained for the three loop master integrals with insertion topology. The labelling of the diagrams is according to Figure 1. The results for the diagrams $A_{5,1}$, $A_{5,2}$, and $A_{6,1}$ can be given for arbitrary propagator powers ν_i. The values of the ν_i are assumed to be such that the arguments of all occurring Γ-functions are different from

$$0, -1, -2, \ldots .$$

In our first diagram, namely $A_{5,1}$, we label the powers of the sloped propagators (i.e. the ones attached to the off-shell leg) by ν_1 and ν_2, whereas ν_3, ν_4, and ν_5 are associated with the three propagators that form the twofold bubble insertion. The form of the diagram immediately suggests that the result must be completely symmetric in $\{\nu_1, \nu_2\}$ as well as in $\{\nu_3, \nu_4, \nu_5\}$. The calculation leads to

$$
\begin{aligned}
A_{5,1}[\nu_i] &= \int \frac{d^D k}{(2\pi)^D} \int \frac{d^D l}{(2\pi)^D} \int \frac{d^D r}{(2\pi)^D} \frac{1}{[(k+p_1)^2]^{\nu_1} [(k-p_2)^2]^{\nu_2} [l^2]^{\nu_3} [(k+l+r)^2]^{\nu_4} [r^2]^{\nu_5}} \\
&= \frac{i \, (-1)^{1-N}}{(4\pi)^{3D/2}} \left[-q^2 - i\eta \right]^{3D/2-N} \frac{\Gamma(\frac{D}{2} - \nu_3) \, \Gamma(\frac{D}{2} - \nu_4) \, \Gamma(\frac{D}{2} - \nu_5)}{\Gamma(\nu_1) \, \Gamma(\nu_2) \, \Gamma(\nu_3) \, \Gamma(\nu_4) \, \Gamma(\nu_5)} \\
&\quad \times \frac{\Gamma(N - \frac{3D}{2}) \, \Gamma(\nu_{345} - D) \, \Gamma(\frac{3D}{2} - N + \nu_1) \, \Gamma(\frac{3D}{2} - N + \nu_2)}{\Gamma(\frac{3D}{2} - \nu_{345}) \, \Gamma(2D - N)} \;,
\end{aligned}
\tag{1}
$$

where we introduced the short-hand notations

$$
\begin{aligned}
\nu_{ijk\ldots} &= \nu_i + \nu_j + \nu_k + \ldots \\
N &= \nu_{12345} \;.
\end{aligned}
\tag{2}
$$

4

In the above equation (1), $\eta > 0$ is an infinitesimal quantity that indicates the way in which the analytical continuation has to be performed in the case $q^2 > 0$.

In the special case in which all ν_i are equal to unity, the result simplifies considerably. Defining a pre-factor S_Γ as

$$S_\Gamma = \frac{1}{(4\pi)^{D/2}\,\Gamma(1-\epsilon)} \ , \tag{3}$$

we have

$$A_{5,1}[\nu_i = 1] \;\; = \;\; i\,S_\Gamma^3\,\left[-\,q^2 - i\,\eta\right]^{1-3\,\epsilon}\,\frac{\Gamma^6(1-\epsilon)\,\Gamma(2\,\epsilon)\,\Gamma(3\,\epsilon)\,\Gamma(1-3\,\epsilon)}{(1-2\,\epsilon)\,(2-3\,\epsilon)\,\Gamma(3-4\,\epsilon)} \ . \tag{4}$$

In the next diagram, $A_{5,2}$, the power of the upper sloped propagator is labelled by ν_1. ν_2 and ν_3 are the powers of the propagators of the lower bubble insertion, whereas ν_4 and ν_5 are associated with the propagators of the vertical bubble. From the form of the diagram we can read off that the result will be symmetric in $\{\nu_2, \nu_3\}$ as well as in $\{\nu_4, \nu_5\}$. It reads

$$
\begin{aligned}
A_{5,2}[\nu_i] \;\; = \;\; & \int\!\frac{d^D k}{(2\pi)^D}\!\int\!\frac{d^D l}{(2\pi)^D}\!\int\!\frac{d^D r}{(2\pi)^D}\,\frac{1}{[(k+p_1)^2]^{\nu_1}\,[(l-k+p_2)^2]^{\nu_2}\,[l^2]^{\nu_3}\,[(k+r)^2]^{\nu_4}\,[r^2]^{\nu_5}} \\[2mm]
= \;\; & \frac{i\,(-1)^{1-N}}{(4\pi)^{3D/2}}\,\left[-\,q^2 - i\,\eta\right]^{3D/2-N}\,\frac{\Gamma(\tfrac{D}{2}-\nu_2)\,\Gamma(\tfrac{D}{2}-\nu_3)\,\Gamma(\tfrac{D}{2}-\nu_4)\,\Gamma(\tfrac{D}{2}-\nu_5)}{\Gamma(\nu_1)\,\Gamma(\nu_2)\,\Gamma(\nu_3)\,\Gamma(\nu_4)\,\Gamma(\nu_5)} \\[2mm]
& \times\,\frac{\Gamma(N-\tfrac{3D}{2})\,\Gamma(D-\nu_{145})\,\Gamma(\nu_{45}-\tfrac{D}{2})\,\Gamma(\tfrac{3D}{2}-N+\nu_1)}{\Gamma(D-\nu_{23})\,\Gamma(D-\nu_{45})\,\Gamma(2D-N)} \ .
\end{aligned} \tag{5}
$$

Again, the case in which all ν_i are equal to unity is much simpler, namely

$$A_{5,2}[\nu_i = 1] \;\; = \;\; -i\,S_\Gamma^3\,\left[-\,q^2 - i\,\eta\right]^{1-3\,\epsilon}\,\frac{\Gamma^7(1-\epsilon)\,\Gamma(\epsilon)\,\Gamma(3\,\epsilon)\,\Gamma(1-3\,\epsilon)}{(1-2\,\epsilon)\,\Gamma(2-2\,\epsilon)\,\Gamma(3-4\,\epsilon)} \ . \tag{6}$$

The last diagram with two bubble insertions is $A_{6,1}$. Again, ν_1 and ν_2 are the powers of the sloped propagators. ν_3 and ν_4 form the powers of the upper bubble insertion, whereas ν_5 and ν_6 are given to the lower one. The diagram also shows several symmetries, namely in $\{\nu_1, \nu_2\}$, $\{\nu_3, \nu_4\}$, $\{\nu_5, \nu_6\}$, and, in addition, in $\{\{\nu_3, \nu_4\}, \{\nu_5, \nu_6\}\}$. One finds

$$
\begin{aligned}
A_{6,1}[\nu_i] \;\; = \;\; & \int\!\frac{d^D k}{(2\pi)^D}\!\int\!\frac{d^D l}{(2\pi)^D}\!\int\!\frac{d^D r}{(2\pi)^D}\,\frac{1}{[(k+p_1)^2]^{\nu_1}\,[(k-p_2)^2]^{\nu_2}} \\[2mm]
& \hspace{5cm} \times\,\frac{1}{[l^2]^{\nu_3}\,[(l+k)^2]^{\nu_4}\,[r^2]^{\nu_5}\,[(r+k)^2]^{\nu_6}} \\[2mm]
= \;\; & \frac{i\,(-1)^{1-N}}{(4\pi)^{3D/2}}\,\left[-\,q^2 - i\,\eta\right]^{3D/2-N}\,\frac{\Gamma(\tfrac{D}{2}-\nu_3)\,\Gamma(\tfrac{D}{2}-\nu_4)\,\Gamma(\tfrac{D}{2}-\nu_5)\,\Gamma(\tfrac{D}{2}-\nu_6)}{\Gamma(\nu_1)\,\Gamma(\nu_2)\,\Gamma(\nu_3)\,\Gamma(\nu_4)\,\Gamma(\nu_5)\,\Gamma(\nu_6)} \\[2mm]
& \times\,\frac{\Gamma(N-\tfrac{3D}{2})\,\Gamma(\nu_{34}-\tfrac{D}{2})\,\Gamma(\nu_{56}-\tfrac{D}{2})\,\Gamma(\tfrac{3D}{2}-N+\nu_1)\,\Gamma(\tfrac{3D}{2}-N+\nu_2)}{\Gamma(D-\nu_{34})\,\Gamma(D-\nu_{56})\,\Gamma(2D-N)} \ ,
\end{aligned} \tag{7}
$$

where this time we have $N = \nu_{123456}$.

Finally, we again give the result for the case in which all ν_i are equal to unity.

$$A_{6,1}[\nu_i = 1] \quad = \quad -i\, S_\Gamma^3 \left[-q^2 - i\,\eta \right]^{-3\,\epsilon} \frac{\Gamma^7(1-\epsilon)\,\Gamma^2(\epsilon)\,\Gamma(3\,\epsilon)\,\Gamma^2(1-3\,\epsilon)}{\Gamma^2(2-2\,\epsilon)\,\Gamma(2-4\,\epsilon)} \quad . \tag{8}$$

Since from now on the diagrams will become more complicated, we restrain ourselves to the case in which the powers of all propagators are equal to unity. The remaining three diagrams to be considered are $A_{6,3}$, $A_{7,1}$, and $A_{7,2}$, each of which contains a single bubble insertion. After integrating out the bubble insertion we are left with an effective two-loop diagram with one propagator less. However, one of the propagators in the effective two-loop graph will carry a power that is different from unity. The two-loop crossed vertex graphs with powers different from unity were discussed previously in [27].

While computing the effective two-loop diagrams, it turns out that, after integrating over the loop momenta, all integrals over Feynman parameters can be carried out in a closed form. The respective results contain Γ-functions in combination with hypergeometric functions of unit argument. We used the aforementioned `Mathematica` package `HypExp` [18] for expanding the all-order results into their respective Laurent series expansions about $\epsilon = 0$. The explicit result for $A_{6,3}$ reads

$$A_{6,3} \quad = \quad \int \frac{d^D k}{(2\pi)^D} \int \frac{d^D l}{(2\pi)^D} \int \frac{d^D r}{(2\pi)^D} \; \frac{1}{k^2\,(k-q)^2\,(k-l)^2\,(l-p_1)^2\,(r-l)^2\,r^2}$$

$$= \quad -i\, S_\Gamma \frac{\Gamma(\epsilon)\,\Gamma^3(1-\epsilon)}{\Gamma(2-2\,\epsilon)} \cdot I_5(\epsilon) \tag{9}$$

with

$$I_5(\alpha) \quad = \quad -(-1)^\alpha \int \frac{d^D k}{(2\pi)^D} \int \frac{d^D l}{(2\pi)^D} \; \frac{1}{k^2\,(k-q)^2\,(k-l)^2\,(l-p_1)^2\,[l^2]^\alpha}$$

$$= \quad S_\Gamma^2 \left[-q^2 - i\,\eta \right]^{-\alpha - 2\,\epsilon} \frac{\Gamma^3(1-\epsilon)\,\Gamma(1-\alpha-\epsilon)\,\Gamma(1-\alpha-2\,\epsilon)}{\Gamma(\alpha)\,\Gamma(2-\alpha-2\,\epsilon)\,\Gamma(2-\alpha-3\,\epsilon)}$$

$$\times \left[\frac{\Gamma(1-\alpha-2\,\epsilon)\,\Gamma(\alpha+2\,\epsilon)\,\Gamma(\alpha+\epsilon)\,\Gamma(\alpha)\,\Gamma(1-\alpha-\epsilon)}{\Gamma(1-\epsilon)} \right.$$

$$\left. + \frac{\Gamma(\alpha+2\,\epsilon-1)\,\Gamma(1-\epsilon)}{(1-2\,\epsilon)} \; {}_3F_2(1, 1-\epsilon, 1-2\,\epsilon\,;\, 2-2\,\epsilon, 2-\alpha-2\,\epsilon\,;\, 1) \right] . \tag{10}$$

Substituting $\alpha = \epsilon$ in Eq. (10) leads to the following series expansion for $A_{6,3}$

$$A_{6,3} \quad = \quad i\, S_\Gamma^3 \left[-q^2 - i\,\eta \right]^{-3\,\epsilon}$$

$$\times \left[-\frac{1}{6\,\epsilon^3} - \frac{3}{2\,\epsilon^2} - \left(\frac{55}{6} + \frac{\pi^2}{6} \right) \frac{1}{\epsilon} - \frac{95}{2} - \frac{3\,\pi^2}{2} + \frac{17\,\zeta_3}{3} \right.$$

$$+\left(-\frac{1351}{6}-\frac{55\,\pi^2}{6}-\frac{\pi^4}{90}+51\,\zeta_3\right)\epsilon$$

$$+\left(-\frac{2023}{2}-\frac{95\,\pi^2}{2}-\frac{\pi^4}{10}+\frac{935\,\zeta_3}{3}+\frac{10\,\pi^2\,\zeta_3}{3}+65\,\zeta_5\right)\epsilon^2$$

$$+\left(-\frac{26335}{6}-\frac{1351\,\pi^2}{6}-\frac{11\,\pi^4}{18}+\frac{7\,\pi^6}{54}\right.$$

$$\left.+1615\,\zeta_3+30\,\pi^2\,\zeta_3-\frac{268\,\zeta_3^2}{3}+585\,\zeta_5\right)\epsilon^3+\mathcal{O}(\epsilon^4)\bigg]\quad.\tag{11}$$

The above Eq. (10) can be used for two other cross-checks. First, we can consider the limit $\alpha\to 0$. This is done by setting $\alpha=\xi\epsilon$, followed by the series expansion in ϵ. Finally, we set $\xi=0$. The result has to coincide – up to a global sign – with the series expansion of the two-loop integral A_4 of Eq. (4) in Ref. [8]. The second check is performed by the limit $\alpha\to 1$, in which case we have to find the result for the two-loop five propagator integral that is obtained from $A_{6,3}$ by removing the bubble. Both checks were found to be fulfilled on the level of the series expansions. The calculation of $I_5(\epsilon)$ by sector decomposition provided an additional check.

We now proceed with the integral $A_{7,1}$, which assumes the form

$$A_{7,1}\;=\;\int\frac{d^D k}{(2\pi)^D}\int\frac{d^D l}{(2\pi)^D}\int\frac{d^D r}{(2\pi)^D}\;\frac{1}{r^2\,(r-k)^2\,(k-q)^2\,(k-l)^2\,(k-l-p_2)^2\,l^2\,(l-p_1)^2}$$

$$=\;-i\,S_\Gamma\,\frac{\Gamma(\epsilon)\,\Gamma^3(1-\epsilon)}{\Gamma(2-2\,\epsilon)}\cdot I_6(\epsilon)\tag{12}$$

with

$$I_6(\alpha)\;=\;-(-1)^\alpha\int\frac{d^D k}{(2\pi)^D}\int\frac{d^D l}{(2\pi)^D}\;\frac{1}{[k^2]^\alpha\,(k-q)^2\,(k-l)^2\,(k-l-p_2)^2\,l^2\,(l-p_1)^2}$$

$$=\;S_\Gamma^2\left[-q^2-i\,\eta\right]^{-1-\alpha-2\,\epsilon}\Gamma^2(1-\epsilon)\,\Gamma^2(-\epsilon)$$

$$\times\left[\frac{\Gamma(-\epsilon)\,\Gamma(2\,\epsilon)}{2\,\Gamma(1-3\,\epsilon)}\,{}_4F_3(\alpha,1-\alpha-4\,\epsilon,1-\epsilon,-2\,\epsilon;1-3\,\epsilon,1-2\,\epsilon,1-2\,\epsilon;1)\right.$$

$$+\frac{\Gamma(1-2\,\epsilon)\,\Gamma(1-\alpha-2\,\epsilon)\,\Gamma(2+\epsilon)\,\Gamma(\alpha+2\,\epsilon)}{\Gamma(\alpha)\,\Gamma(2-\epsilon)\,\Gamma(1-\alpha-4\,\epsilon)}$$

$$\times{}_4F_3(1,1,1-2\,\epsilon,2+\epsilon;2,2,2-\epsilon;1)$$

$$-\frac{2\,\Gamma(-2\,\epsilon)\,\Gamma(1+\alpha+2\,\epsilon)\,\Gamma(2+\epsilon)\,\Gamma(1-\alpha-2\,\epsilon)}{\Gamma(\alpha)\,\Gamma(2-\epsilon)\,\Gamma(1-\alpha-4\,\epsilon)}$$

$$\times{}_4F_3(1,1,1+\alpha+2\,\epsilon,2+\epsilon;2,2,2-\epsilon;1)$$

$$-\frac{\Gamma(\alpha+2\,\epsilon)\,\Gamma(2-\alpha-\epsilon)}{(1-\alpha-2\,\epsilon)^2\,\Gamma(\alpha)\,\Gamma(2-\alpha-3\,\epsilon)}$$

$$\times {}_4F_3(1, 1 - \alpha - 2\,\epsilon, 1 - \alpha - 4\,\epsilon, 2 - \alpha - \epsilon\,;\, 2 - \alpha - 2\,\epsilon, 2 - \alpha - 2\,\epsilon, 2 - \alpha - 3\,\epsilon\,;\, 1)$$

$$+ \frac{\Gamma(-2\,\epsilon)\,\Gamma(1 + 2\,\epsilon)\,\Gamma(2 + \epsilon)\,\Gamma(1 + \alpha + 2\,\epsilon)\,\Gamma(2 - \alpha - 2\,\epsilon)}{\Gamma(\alpha)\,\Gamma(1 - \alpha - 4\,\epsilon)\,\Gamma(2 - \epsilon)\,\Gamma(2 + 2\,\epsilon)}$$

$$\times \left. {}_5F_4(1, 1, 2 - \alpha - 2\,\epsilon, 1 + \alpha + 2\,\epsilon, 2 + \epsilon\,;\, 2, 2, 2 - \epsilon, 2 + 2\,\epsilon\,;\, 1) \right] . \tag{13}$$

Again, we have to set $\alpha = \epsilon$ in Eq. (13) in order to obtain the series expansion for $A_{7,1}$. It reads

$$A_{7,1} = i\, S_\Gamma^3 \left[-q^2 - i\,\eta \right]^{-1-3\,\epsilon}$$

$$\times \left[\frac{1}{4\,\epsilon^5} + \frac{1}{2\,\epsilon^4} + \left(1 - \frac{\pi^2}{6} \right) \frac{1}{\epsilon^3} + \left(2 - \frac{\pi^2}{3} - 10\,\zeta_3 \right) \frac{1}{\epsilon^2} \right.$$

$$+ \left(4 - \frac{2\,\pi^2}{3} - \frac{11\,\pi^4}{45} - 20\,\zeta_3 \right) \frac{1}{\epsilon}$$

$$+ \left(8 - \frac{4\,\pi^2}{3} - \frac{22\,\pi^4}{45} - 40\,\zeta_3 + \frac{14\,\pi^2\,\zeta_3}{3} - 88\,\zeta_5 \right)$$

$$+ \left(16 - \frac{8\,\pi^2}{3} - \frac{44\,\pi^4}{45} - \frac{943\,\pi^6}{7560} - 80\,\zeta_3 \right.$$

$$\left. \left. + \frac{28\,\pi^2\,\zeta_3}{3} + 196\,\zeta_3^2 - 176\,\zeta_5 \right) \epsilon + \mathcal{O}(\epsilon^2) \right] . \tag{14}$$

The integral $I_6(\alpha)$ provides another cross check since for $\alpha = 1$ we have to reproduce the integral A_6 of Eq. (5) in Ref. [8]. This we checked to be the case on the level of the series expansion.

As we proceed, the expressions for the integrals become more and more lengthy. The result for the integral $A_{7,2}$ reads

$$A_{7,2} = \int \frac{d^D k}{(2\pi)^D} \int \frac{d^D l}{(2\pi)^D} \int \frac{d^D r}{(2\pi)^D} \frac{1}{k^2\,(k-q)^2\,(l-p_1)^2\,(k-l)^2\,(k-l-p_2)^2\,r^2\,(r-l)^2}$$

$$= -i\, S_\Gamma \frac{\Gamma(\epsilon)\,\Gamma^3(1-\epsilon)}{\Gamma(2 - 2\,\epsilon)} \cdot J_6(\epsilon) \tag{15}$$

with

$$J_6(\alpha) = -(-1)^\alpha \int \frac{d^D k}{(2\pi)^D} \int \frac{d^D l}{(2\pi)^D} \frac{1}{k^2\,[l^2]^\alpha\,(k-q)^2\,(l-p_1)^2\,(k-l)^2\,(k-l-p_2)^2}$$

$$= S_\Gamma^2 \left[-q^2 - i\,\eta \right]^{-1-\alpha-2\,\epsilon} \Gamma(1 - \epsilon)\,\Gamma(-\epsilon)\,\Gamma(1 - \alpha - \epsilon)$$

$$\times \left[- \frac{\Gamma(1 - \alpha - 2\,\epsilon)\,\Gamma(\alpha + \epsilon)\,\Gamma(\alpha + 2\,\epsilon)\,\Gamma(1 - \epsilon)\,\Gamma(-\epsilon)\,\Gamma^2(\epsilon)}{4\,\Gamma(\alpha)\,\Gamma(1 - \alpha - 4\,\epsilon)\,\Gamma(2\,\epsilon)} \right.$$

$$+\frac{\Gamma(1-\alpha-2\,\epsilon)\,\Gamma(\alpha+\epsilon)\,\Gamma(\alpha+2\,\epsilon)\,\Gamma(-2\,\epsilon)}{\epsilon\,\Gamma(\alpha)\,\Gamma(1-\alpha-4\,\epsilon)}$$

$$-\frac{\Gamma^2(1-\alpha-2\,\epsilon)\,\Gamma(\alpha+\epsilon)\,\Gamma^2(\alpha+2\,\epsilon)\,\Gamma(\alpha+4\,\epsilon)}{\Gamma(\alpha)\,\Gamma(1+2\,\epsilon)}$$

$$-\frac{\Gamma(1-\alpha-2\,\epsilon)\,\Gamma(1-\epsilon)\,\Gamma(\alpha+\epsilon)\,\Gamma(\alpha+2\,\epsilon-1)}{\Gamma(\alpha)\,\Gamma(2-\alpha-3\,\epsilon)}$$
$$\times\,{}_3F_2(1,1-\alpha-2\,\epsilon,1-\alpha-4\,\epsilon\,;\,2-\alpha-2\,\epsilon,2-\alpha-3\,\epsilon\,;\,1)$$
$$+\frac{\Gamma(\alpha-1)\,\Gamma(1-\alpha-2\,\epsilon)\,\Gamma(1-\epsilon)\,\Gamma(-2\,\epsilon)\,\Gamma(1+\epsilon)\,\Gamma(1+2\,\epsilon)}{\Gamma(\alpha)\,\Gamma(1-\alpha-4\,\epsilon)\,\Gamma(2-\alpha-\epsilon)}$$
$$\times\,{}_3F_2(1-\alpha,1+\epsilon,1+2\,\epsilon\,;\,2-\alpha,2-\alpha-\epsilon\,;\,1)$$
$$+\frac{\Gamma(1-\epsilon)\,\Gamma(-2\,\epsilon)\,\Gamma(1+\epsilon)\,\Gamma(1+2\,\epsilon)\,\Gamma(\alpha+\epsilon)\,\Gamma(\alpha+2\,\epsilon)}{(\alpha+4\,\epsilon)\,\Gamma(\alpha)\,\Gamma(1-\alpha-3\,\epsilon)\,\Gamma(1+\alpha+3\,\epsilon)}$$
$$\times\,{}_3F_2(1+\epsilon,1+2\,\epsilon,\alpha+4\,\epsilon\,;\,1+\alpha+3\,\epsilon,1+\alpha+4\,\epsilon\,;\,1)$$
$$+\frac{\Gamma(1-2\,\epsilon)\,\Gamma(1-\alpha-2\,\epsilon)\,\Gamma(1-\epsilon)\,\Gamma(1+\alpha+\epsilon)\,\Gamma(\alpha+2\,\epsilon)}{\Gamma(1+\alpha)\,\Gamma(1-\alpha-4\,\epsilon)\,\Gamma(2-\epsilon)}$$
$$\times\,{}_4F_3(1,1,1-2\,\epsilon,1+\alpha+\epsilon\,;\,2,1+\alpha,2-\epsilon\,;\,1)$$
$$+\frac{\Gamma^2(1-\epsilon)\,\Gamma(2\,\epsilon)\,\Gamma(\alpha+\epsilon)\,\Gamma(\alpha+2\,\epsilon)}{(\alpha+2\,\epsilon)\,\Gamma(\alpha)\,\Gamma(1-\alpha-3\,\epsilon)\,\Gamma(1+\alpha+\epsilon)\,\Gamma(1+2\,\epsilon)}$$
$$\times\,{}_4F_3(1,1,1-\epsilon,\alpha+2\,\epsilon\,;\,1-2\,\epsilon,1+\alpha+\epsilon,1+\alpha+2\,\epsilon\,;\,1)$$
$$+\frac{\Gamma(1-\alpha-2\,\epsilon)\,\Gamma^2(1-\epsilon)\,\Gamma(\alpha+2\,\epsilon-1)}{\Gamma(2-\alpha-3\,\epsilon)\,\Gamma(1-2\,\epsilon)}$$
$$\times\,{}_4F_3(1,1-\alpha-4\,\epsilon,1-\alpha-2\,\epsilon,1-\epsilon\,;\,2-\alpha-2\,\epsilon,2-\alpha-3\,\epsilon,1-2\,\epsilon\,;\,1)$$
$$+\frac{\alpha\,\Gamma(1-\alpha-2\,\epsilon)\,\Gamma(-2\,\epsilon)\,\Gamma(\alpha+\epsilon)\,\Gamma(\alpha+2\,\epsilon)}{\Gamma(\alpha)\,\Gamma(1-\alpha-4\,\epsilon)}\,{}_3F_2(1,1,1+\alpha\,;\,2,2\,;\,1)$$
$$-\frac{\Gamma(1-\alpha-2\,\epsilon)\,\Gamma(-2\,\epsilon)\,\Gamma(\alpha+\epsilon)\,\Gamma(1+\alpha+2\,\epsilon)}{\Gamma(\alpha)\,\Gamma(1-\alpha-4\,\epsilon)}$$
$$\times\,{}_3F_2(1,1,1+\alpha+2\,\epsilon\,;\,2,2\,;\,1)\Big]\,. \tag{16}$$

Details about the calculation of Eq. (16) can be found in Ref. [28]. Useful formulas that got applied at intermediate steps were taken from Refs. [29–31]. Setting $\alpha=\epsilon$ leads to the following series expansion of $A_{7,2}$,

$$
\begin{aligned}
A_{7,2} \;=\;\; & i\,S_\Gamma^3\left[-q^2-i\,\eta\right]^{-1-3\,\epsilon}\\[4pt]
& \times\left[\frac{\pi^2}{12\,\epsilon^3}+\left(\frac{\pi^2}{6}+2\,\zeta_3\right)\frac{1}{\epsilon^2}+\left(\frac{\pi^2}{3}+\frac{83\,\pi^4}{720}+4\,\zeta_3\right)\frac{1}{\epsilon}\right.\\[4pt]
& \left.\qquad+\left(\frac{2\,\pi^2}{3}+\frac{83\,\pi^4}{360}+8\,\zeta_3-\frac{5\,\pi^2\,\zeta_3}{3}+15\,\zeta_5\right)\right.
\end{aligned}
$$

9

$$+ \left(\frac{4\,\pi^2}{3} + \frac{83\,\pi^4}{180} + \frac{2741\,\pi^6}{90720} + 16\,\zeta_3 \right.$$

$$\left. - \frac{10\,\pi^2\,\zeta_3}{3} - 73\,\zeta_3^2 + 30\,\zeta_5 \right) \epsilon + \mathcal{O}(\epsilon^2) \Bigg] \quad . \tag{17}$$

We finally state that the expression (16) for $J_6(\alpha)$ can again be used for several cross checks. First, in the limit $\alpha \to 1$ we have to obtain the same result as for A_6 of Eq. (5) in Ref. [8] or $I_6(1)$ of Eq. (13). The check is done by first considering $\alpha = 1 + \chi\,\epsilon$ in (16) followed by a subsequent expansion in ϵ. In the end, the limit $\chi \to 0$ is carried out. A second check is provided by the limit $\alpha \to 0$. We again set $\alpha = \eta\,\epsilon$ and carry out the series expansion, followed by letting $\eta \to 0$. The result has to be the same – up to a global sign – as the series expansion of $I_5(1)$ of Eq. (10). All checks have been verified on the level of the respective Laurent series.

As mentioned earlier, the coefficients of the Laurent series are real numbers. Therefore the method of sector decomposition is particularly well suited to compute the coefficients numerically, thereby providing the most important check of our analytical findings.

5   Conclusions

In this letter, we identified and classified the master integrals required for a calculation of the massless three-loop quark and gluon form factors. In addition to three-loop two-point functions and products of one-loop and two-loop integrals, we identified 16 genuine three-loop vertex integrals, which are displayed in Figure 1. Among these, six integrals are so-called insertion graphs, containing a bubble insertion into a one-loop or two-loop vertex graph. We computed the master integrals for these insertion graphs analytically in a closed form which is exact to all orders in ϵ, containing Γ-functions and hypergeometric functions. Laurent series expansions were subsequently obtained using the `HypExp`-package. All Laurent series expansions were verified independently using sector decomposition to determine the expansion coefficients numerically.

The remaining ten master integrals do not contain subtopologies which would allow us to relate them to two-loop integrals. Their analytical computation may not be possible using Feynman parameters, but appears feasible with modern loop-integral techniques [32], such as Mellin-Barnes integration [33]. Using sector decomposition, their Laurent expansion can be obtained in a straightforward manner.

Acknowledgements

References

[1] S. Catani, Phys. Lett. B **427** (1998) 161 [hep-ph/9802439].

[2] G. Sterman and M.E. Tejeda-Yeomans, Phys. Lett. B **552** (2003) 48 [hep-ph/0210130].

[3] S. Moch, J.A.M. Vermaseren and A. Vogt, JHEP **0508** (2005) 049 [hep-ph/0507039].

[4] G. Kramer and B. Lampe, Z. Phys. C **34** (1987) 497; **42** (1989) 504(E);
T. Matsuura and W.L. van Neerven, Z. Phys. C **38** (1988) 623;
T. Matsuura, S.C. van der Maarck and W.L. van Neerven, Nucl. Phys. B **319** (1989) 570.

[5] R.V. Harlander, Phys. Lett. B **492** (2000) 74 [hep-ph/0007289].

[6] V. Ravindran, J. Smith and W.L. van Neerven, Nucl. Phys. B **704** (2005) 332 [hep-ph/0408315].

[7] W. Bernreuther *et al.*, Nucl. Phys. B **706** (2005) 245 [hep-ph/0406046]; Nucl. Phys. B **712** (2005) 229 [hep-ph/0412259]; Nucl. Phys. B **723** (2005) 91 [hep-ph/0504190].

[8] T. Gehrmann, T. Huber and D. Maître, Phys. Lett. B **622** (2005) 295 [hep-ph/0507061].

[9] S. Moch, J.A.M. Vermaseren and A. Vogt, Phys. Lett. B **625** (2005) 245 [hep-ph/0508055].

[10] S. Moch and A. Vogt, Phys. Lett. B **631** (2005) 48 [hep-ph/0508265].

[11] J.A.M. Vermaseren, A. Vogt and S. Moch, Nucl. Phys. B **724** (2005) 3 [hep-ph/0504242].

[12] F.V. Tkachov, Phys. Lett. **100B** (1981) 65;
K.G. Chetyrkin and F.V. Tkachov, Nucl. Phys. **B192** (1981) 159.

[13] S. Laporta, Int. J. Mod. Phys. A **15** (2000) 5087 [hep-ph/0102033].

[14] T. Gehrmann and E. Remiddi, Nucl. Phys. B **580** (2000) 485 [hep-ph/9912329].

[15] C. Anastasiou and A. Lazopoulos, JHEP **0407** (2004) 046 [hep-ph/0404258].

[16] P.A. Baikov, Phys. Lett. B **634** (2006) 325 [hep-ph/0507053].

[17] P.A. Baikov, K.G. Chetyrkin and J.H. Kühn, Phys. Rev. Lett. **96** (2006) 012003 [hep-ph/0511063].

[18] T. Huber and D. Maître, Comput. Phys. Commun. **175** (2006) 122 [hep-ph/0507094].

[19] S. Moch and P. Uwer, Comput. Phys. Commun. **174** (2006) 759 [math-ph/0508008].

[20] S. Bekavac, hep-ph/0505174.

[21] S.G. Gorishnii, S.A. Larin, L.R. Surguladze and F.V. Tkachov, Comput. Phys. Comm. **55** (1989) 381;
S.A. Larin, F.V. Tkachov and J.A.M. Vermaseren, NIKHEF-H-91-18.

[22] P. Marquard, J. H. Piclum, D. Seidel and M. Steinhauser, hep-ph/0607168.

[23] R.J. Gonsalves, Phys. Rev. **D28** (1983) 1542;
G. Kramer and B. Lampe, J. Math. Phys. **28** (1987) 945.

[24] *MATHEMATICA* 5.2, Copyright 2005 by Wolfram Research.

[25] T. Binoth and G. Heinrich, Nucl. Phys. B **585** (2000) 741 [hep-ph/0004013].

[26] T. Binoth and G. Heinrich, Nucl. Phys. B **680** (2004) 375 [hep-ph/0305234].

[27] S. Moch, Nucl. Instrum. Meth. A **559** (2006) 285 [math-ph/0509058].

[28] C. Studerus, B.Sc. Thesis, University of Zürich (2006), in German.

[29] A. Erdélyi (ed.), Higher transcendental functions, Vol. 1, (McGraw-Hill, New York, 1953) .

[30] A. Erdélyi (ed.), Tables of Integral Transforms, Vol. 2, (McGraw-Hill, New York, 1954) .

[31] `http://functions.wolfram.com`.

[32] V. A. Smirnov, *"Evaluating Feynman integrals"*, Springer Tracts Mod. Phys. **211** (2004) 1.

[33] V.A. Smirnov, Phys. Lett. B **460** (1999) 397 [hep-ph/9905323];
J.B. Tausk, Phys. Lett. B **469** (1999) 225 [hep-ph/9909506].